NASA Contractor Report 195307

Control Strategies for Systems With Limited Actuators

Vincent R. Marcopoli and Stephen M. Phillips
Case Western Reserve University
Cleveland, Ohio

April 1994

Prepared for
Lewis Research Center
Under Grant NAG3–1232

National Aeronautics and
Space Administration

Control Strategies for Systems With Limited Actuators

REPORT AND PROPOSAL FOR NASA GRANT NAG3-1232

Vincent R. Marcopoli and Stephen M. Phillips

Department of Electrical Engineering and Applied Physics
Case Western Reserve University
Cleveland, OH 44106

December 10, 1993

Abstract

This work investigates the effects of actuator saturation in multi-input, multi-output (MIMO) control systems. The adverse system behavior introduced by the saturation nonlinearity is viewed here as resulting from two mechanisms: 1) Controller windup — a problem caused by the discrepancy between the limited actuator commands and the corresponding control signals, and 2) Directionality — the problem of how to use *nonlimited* actuators when a limited condition exists. The tracking mode and Hanus methods are two common strategies for dealing with the windup problem. It is seen that while these methods alleviate windup, performance problems remain due to plant directionality. Though high gain conventional antiwindup as well as more general linear methods have the potential to address both windup and directionality, no systematic design method for these schemes has emerged; most approaches used in practice are application driven. An alternative method of addressing the directionality problem is presented which involves the introduction of a control direction preserving nonlinearity to the Hanus antiwindup system. A nonlinearity is subsequently proposed which reduces the conservatism inherent in the former direction-preserving approach, improving performance. The concept of multivariable sensitivity is seen to play a key role in the success of the new method.

Part I

Grant Report

1 Introduction

Nearly all practical control problems involve plants whose actuators are limited by inherent physical constraints. Examples include constraints on valve openings in chemical process control; motor current in servomechanism control; flight control surface angle deflections, engine nozzle openings, and fuel flows in aerospace systems. These constraints are often modeled by a saturation nonlinearity operating on the controller output, as shown in Figure 1. In the multi-input, multi-output (MIMO) case, the saturation block represents decoupled saturation nonlinearities applied to each component of the controller output vector, u_c, producing the effective plant actuator signal, u_a. More formally, this nonlinear operation is defined component-wise as follows:

$$u_{a,i} = \text{sat}(u_{c,i}),\ i = 1 \ldots m,$$

where

$$\text{sat}(u_{c,i}) = \begin{cases} u_{c,i} & , \ |u_{c,i}| \leq L_i \\ L_i \,\text{sgn}(u_{c,i}) & , \ |u_{c,i}| > L_i \end{cases},$$

m is the number of actuators, and L_i is the limit value of the i'th actuator. The effect of this simple nonlinearity on system performance can be quite significant, especially in the MIMO situation. To illustrate this problem, consider the following two-input, two-output linear control systems.

System S1: SISO

$$P = \frac{s+1}{s+0.5},\ K = \frac{20}{s+0.8}$$

The nominal response of this system is shown in Figure 2, where the plant output, y, and the corresponding actuator command signal, $u_a = u_c$, are shown. The response of the limited system with $L_1 = 0.7$ is shown in Figure 3, where it is seen that the plant output now overshoots its desired steady-state value of $y = 1$ (dashed line). Note that u_a (solid line) and u_c (dashed line) are significantly different during limiting conditions. This discrepancy between u_a and u_c is shown in Section 2 to be the cause of the adverse behavior of y.

System M1: MIMO [DSE87]

$$P = \frac{4(0.1+s)}{s}\begin{bmatrix} 4 & -5 \\ -3 & 4 \end{bmatrix},\ K = \frac{1}{4(0.1+s)}\begin{bmatrix} 4 & 5 \\ 3 & 4 \end{bmatrix}$$

This is an inverse-model based control system, designed for the decoupled closed loop response $H_{cr} = \frac{s}{s+1}I$. The nominal response to a step reference command, $r_1 = [0.615\ 0.788]^T$, is shown in Figure 4, where y_1 (solid line) and y_2 (dashed line) are depicted in the upper plot, and u_1 (solid line) and u_2 (dashed line) are shown in the lower plot. The output responses for the limited actuator system are shown similarly in Figure 5, where $L_1 = L_2 = 1$. The controller output, $u_{c,1}$ (dotted line), is further shown to be very different from the true actuator command, $u_{a,1}$. Comparing qualitatively Figure 5 with Figure 3 illustrates that saturation in MIMO systems can cause even more troublesome behavior than in the SISO case.

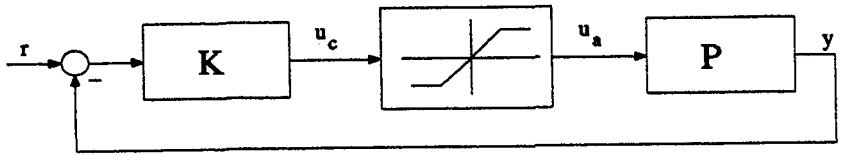

Figure 1: Limited closed loop system

System M2: MIMO [CM90]

$$P = \frac{1}{10s+1}\begin{bmatrix} 4 & -5 \\ -3 & 4 \end{bmatrix}, \; K = \frac{10s+1}{s}\begin{bmatrix} 4 & 5 \\ 3 & 4 \end{bmatrix}$$

This system yields a decoupled closed loop response identical to that of system M1. The key difference is that the controller here is proper (i.e. has a direct feedthrough, or D term, in its realization), whereas that given in system M1 is strictly proper. This difference in controller structure will be shown in the sequel to be a significant factor in determining how the limit problem will be accommodated. The nominal and limited ($L_1 = L_2 = 15$) responses are shown in Figures 6 and 7, respectively, for the reference step $r_2 = [0.315 \; -0.949]^T$. Note again the dramatic effect that limits have on this system, both during the time when the limits are in effect, and long after they cease.

Since most control design methods allow or require specifications on actuator effort, one way to prevent an actuator saturation from occurring would be to explicitly design the controller so that its actuator commands never violate the limits for any expected reference commands. While this approach avoids the problems that limits introduce into the system, performance is usually compromised when operating well within the limits.

A commonly used alternative approach to this problem employs a two-step design procedure. First, a control design is performed on the system to yield a system with desired closed-loop properties in the absence of actuator limits. Many physical considerations are likely to be used in this design, including actuator limits to establish relative sizes of the actuator commands. However, the limits are not considered when evaluating the resulting system performance. This procedure defines what will be referred to as the *nominal* system. All nominal systems considered here are linear.

The second step in this procedure is to modify the nominal control scheme if and only if limits are in effect. In other words, the modified controller should exactly reduce to the nominal controller when limited conditions do not exist. The goal of the modified controller is to provide for *graceful performance degradation* when limits occur. This refers to the fact that when limits take effect, some performance degradation must be accepted. However, Figures 5 and 7 illustrate that in the absence of controller modification under limited conditions, the degraded performance may not even closely resemble that of the nominal system. The goal of graceful performance degradation is one of maintaining the *qualitative* system behavior under limited conditions, with the degradation appearing in some well-defined, predictable manner (e.g. slower responses).

This document consists of both the grant report (Part I) and proposal (Part II). The remainder of Part I intends to: 1) Motivate and present several schemes which have been successful in combating particular instances of performance degradation commonly associated with limited feedback systems, and 2) present preliminary results which suggest improvements upon existing methods. Specifically, in Section 2, the notion of controller windup is presented, along with three common methods of alleviating it. Section 3 presents an additional aspect of the problem, introduced in [DSE87], which is unique to MIMO systems: Performance degradation due to plant directionality. It is this characteristic of limited MIMO systems which presents the most difficulty in achieving graceful performance degradation. In Section 3.1, a solution to this problem,

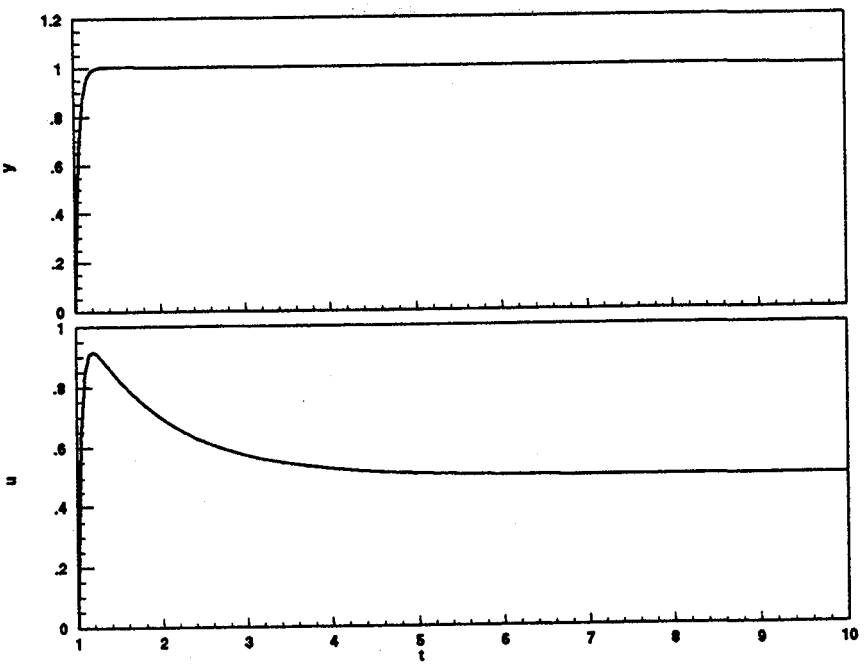

Figure 2: System S1 nominal step response

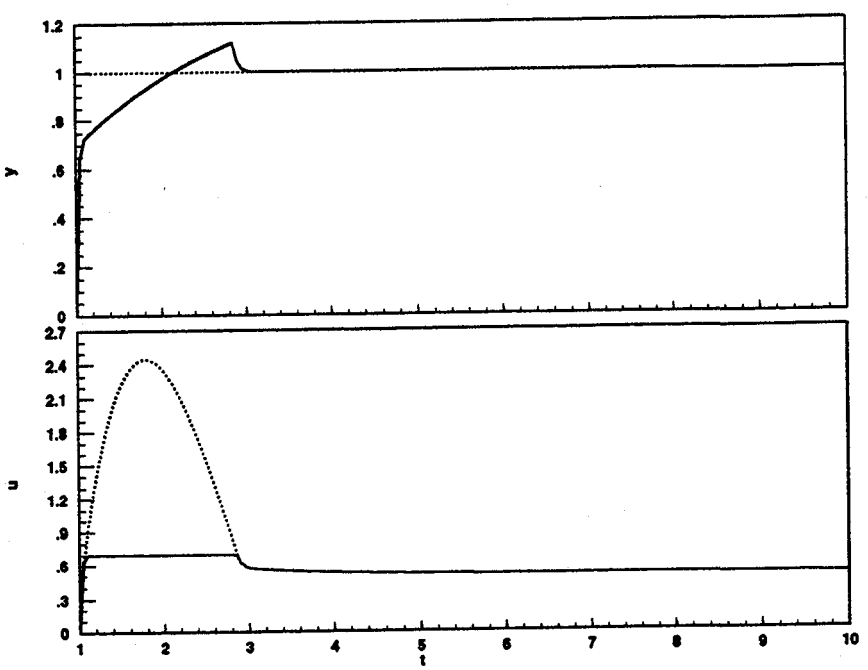

Figure 3: System S1 limited step response

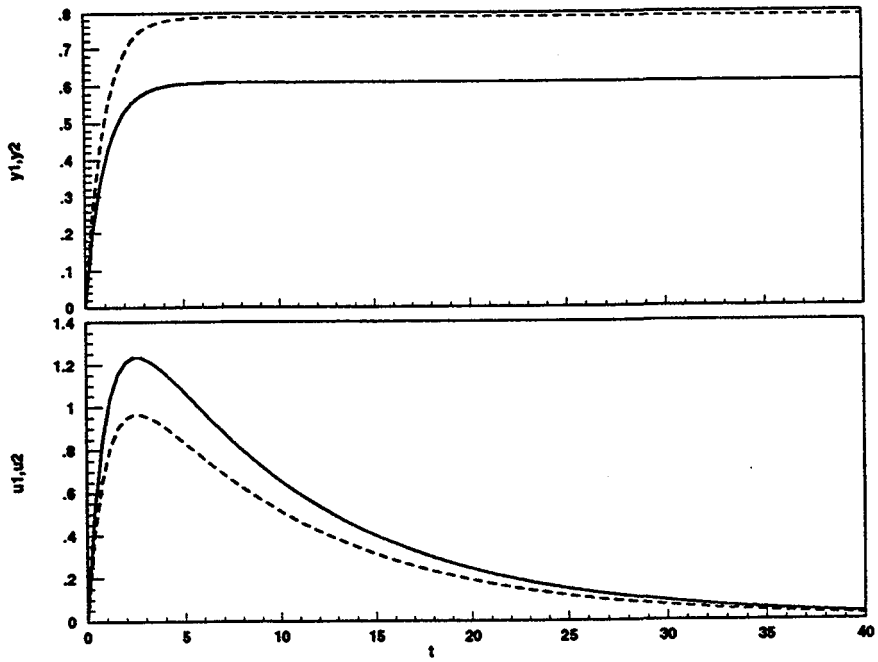

Figure 4: System M1 nominal step response

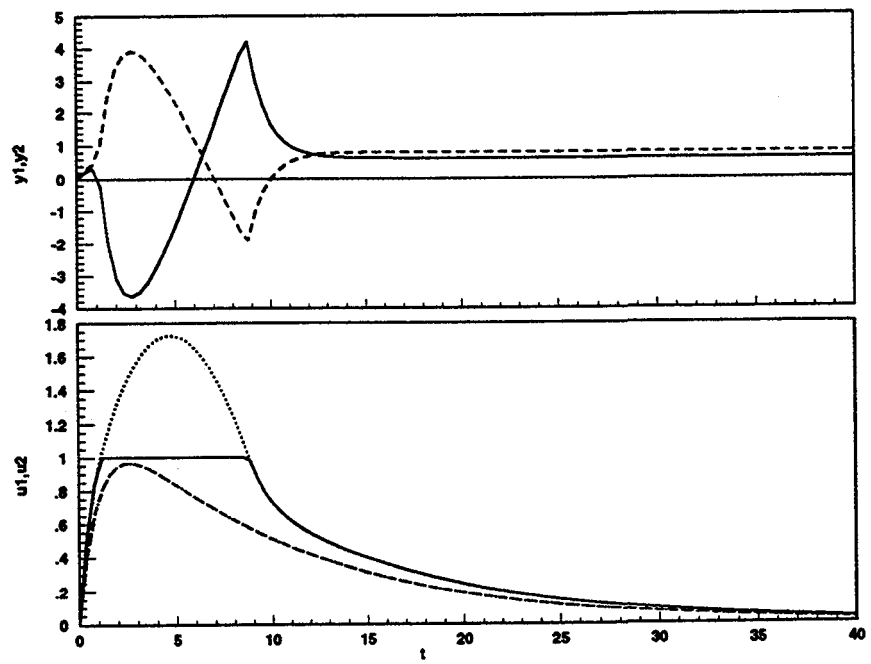

Figure 5: System M1 limited step response

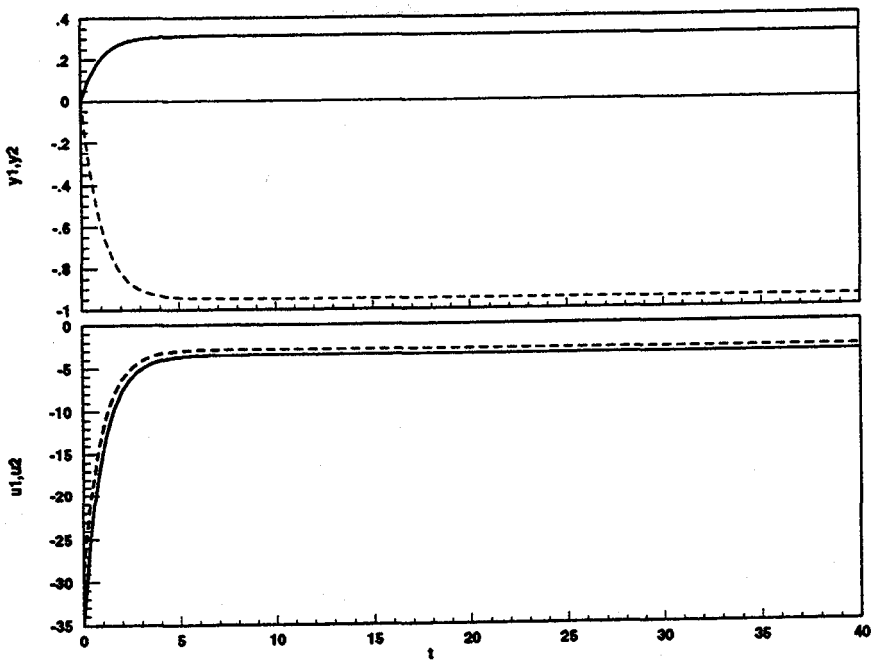

Figure 6: System M2 limited step response

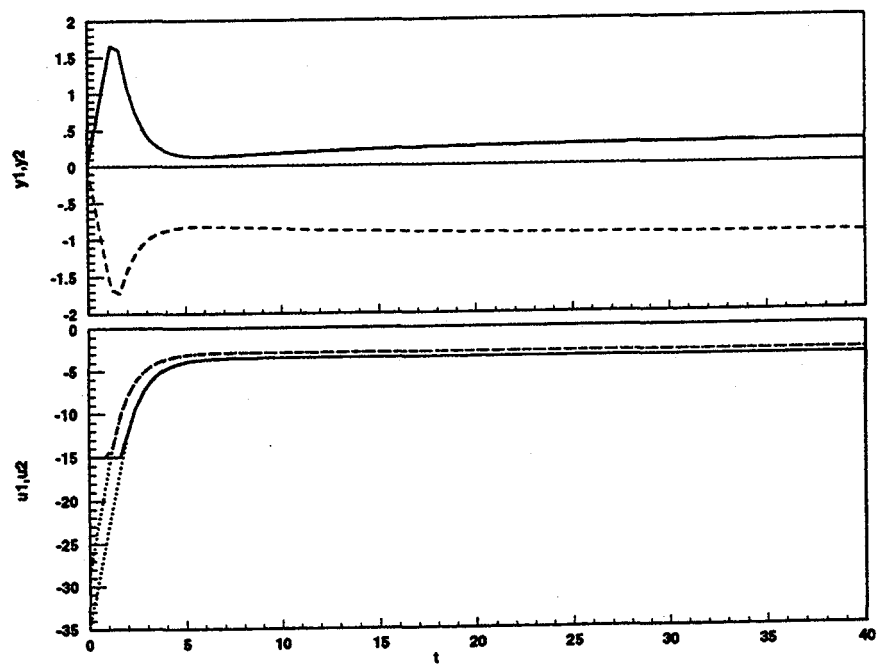

Figure 7: System M2 limited step response

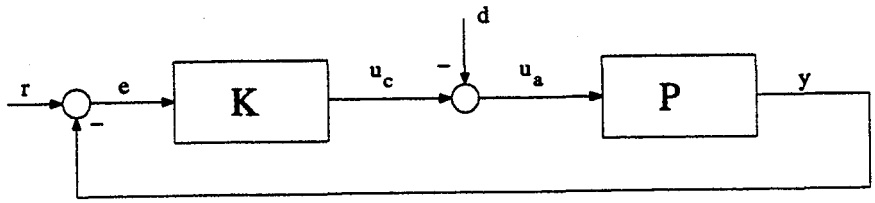

Figure 8: Nominal system with plant input disturbance

developed in [CM90], is presented. Sections 3.2 and 3.3 contain the particular contributions of this research, where improvements to the method of Section 3.1 are proposed, providing new insight into the directionality problem. Finally, Part II discusses future goals of this research.

2 Controller Windup

When an actuator is limited, it is effectively removed from the feedback loop. In this situation, the controller output is inconsistent with the plant input, and the plant output does not have its usual meaning as a feedback signal. When the controller contains integrators or slow dynamics (i.e. has long "memory"), this incorrect feedback can negatively impact performance both during, and long after the limited condition ceases. This phenomenon is commonly known as *windup* or *integrator windup*.

More specifically, refer to the limited system of Figure 1, and model the saturation nonlinearity as a plant input disturbance to the nominal closed loop system, as shown in Figure 8. Thus $u_a = u_c - d$, $y = Pu_c - Pd$, and the error signal produced is $e = r - Pu + Pd$. The resulting controller output is therefore

$$u_c = K(r - Pu_c) + KPd$$

Note that the first term above is in fact the control signal that would occur in the absence of limits. The second term is due to the limiting process, and identifies d, the discrepancy between u_c and u_a, along with the *open loop* dynamics KP as determining the nature of the windup effects. As discussed in the introduction, the approach taken here to combat windup effects is to appropriately modify the controller under limiting conditions. The remainder of this section presents three common methods of doing this.

2.1 Conventional Antiwindup (CAW)

A solution to the above problem which has been effective in many situations is the so-called "high gain conventional antiwindup" approach, shown in Figure 9. In this method, the difference between the controller output and the plant input is fed back through a large static gain in addition to the plant output. This new loop prevents windup by overriding the erroneous feedback of the plant output in favor of making the controller output approach the plant input. This can be seen by breaking the system of Figure 9 at the saturation block, and solving for u_c:

$$u_c = (I + KX)^{-1}Kr + (I + KX)^{-1}KXu_a - (I + KX)^{-1}KPu_a$$

By choosing X such that the gain and bandwidth of KX are large with respect to K and KP (e.g. $\underline{\sigma}(KX) \gg \overline{\sigma}(K)$ and $\underline{\sigma}(KX) \gg \overline{\sigma}(KP)$), the above expression approximates $u_c = u_a$. In the literature, this has been called a *tracking mode* of controller operation. Windup is alleviated here by providing for consistency between controller output and plant input under limited conditions.

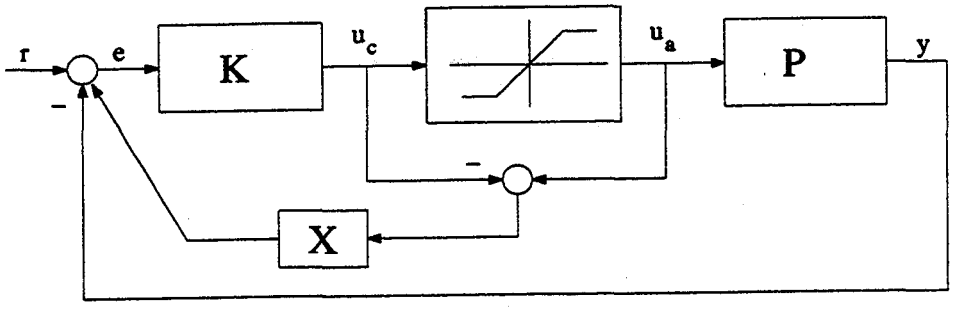

Figure 9: Conventional antiwindup scheme

Note that the static gain causes this action to be taken if *and only if* limited conditions exist (i.e. u_a differs from u_c). When $u_c = u_a$ the antiwindup gain has no effect on the nominal controller. This is a fundamental characteristic of an effective antiwindup mechanism as stated in Section 1, guaranteeing that nominal performance will be recovered when limited conditions cease.

Further insight into the selection of X is gained by examining the system of Figure 9 using the state space controller description. Assume the nominal controller has the following realization:

$$\begin{aligned} \dot{x} &= Ax + Be \\ u_c &= Cx \end{aligned}$$

Substituting $e = r - y + X(u_a - u_c)$ and simplifying yields:

$$\dot{x} = (A - BXC)x + B(r - y) + BXu_a$$

Note that when $u_a = u_c = Cx$, the above equation reduces to the nominal case. When $u_a \neq u_c$, windup effects can be alleviated by implementing a tracking mode of u_c to u_a. This can be done heuristically by choosing X such that the last term dominates the second term. For any choice of X to work, it must further be verified that stability will be maintained under limited conditions. It is shown in [CMN89] that a sufficient condition for nonlinear stability is that $(A - BXC)$ be stable.

Figure 10 depicts the response of system S1 using the CAW approach with $X = 10$. The overshoot in y due to windup has been eliminated. how the control signal has been affected to achieve The improved response is due to tracking behavior of the control signal, u_c (dotted line), to the limited actuator command, u_a (solid line). It is this consistency between the plant input and controller output which eliminates the windup effects.

2.2 Generalized MIMO Antiwindup

The MIMO antiwindup problem is cast in a more general framework in [CMN89]. A version of this approach which is sufficient for the current discussion is shown in Figure 11. Assume the nominal controller has the following state space realization:

$$\begin{aligned} \dot{x} &= Ax + Be \\ u_c &= Cx + De. \end{aligned}$$

The "augmented" controller shown in Figure 11 has the realization

$$\dot{x} = Ax + Be + \Lambda(u_a - u_c) \quad (1)$$

$$u_c = Cx + De \quad (2)$$

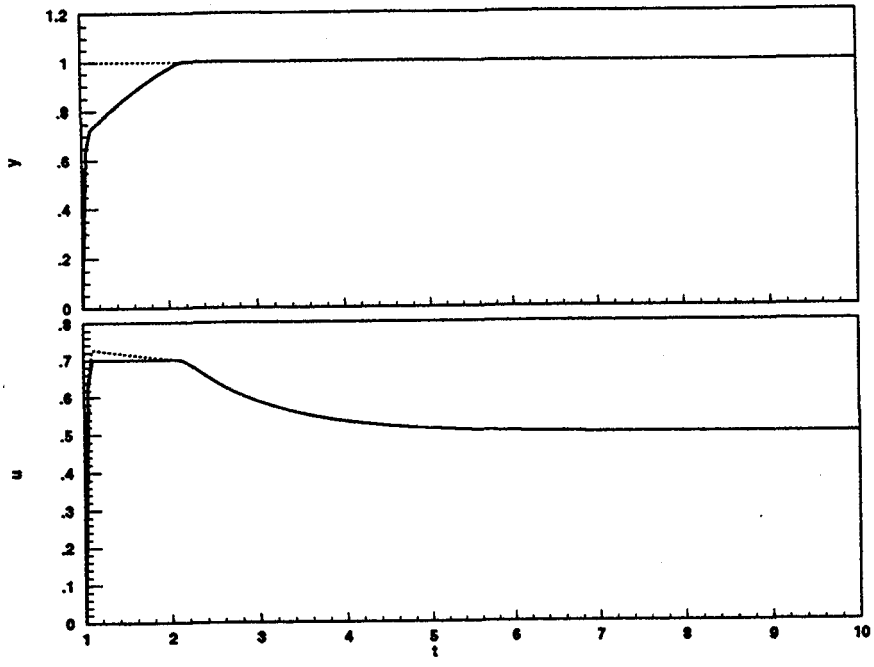

Figure 10: System S1 CAW step response

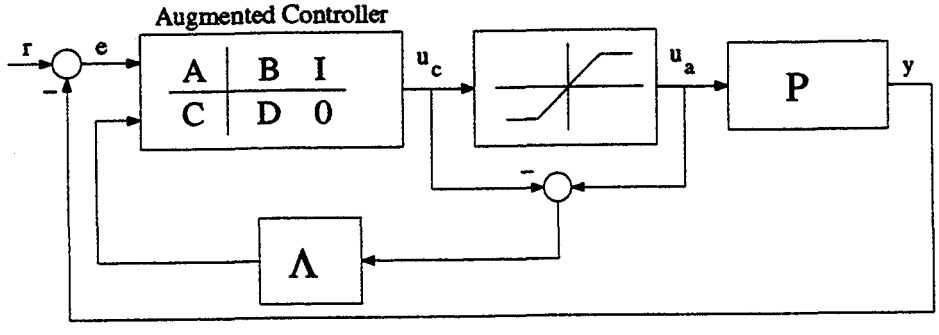

Figure 11: Generalized antiwindup scheme

Note that this differs from the CAW approach (Figure 9) in that here, the actuator error, $(u_a - u_c)$, directly alters the states of the controller (via Λ), whereas in CAW, the actuator error affects the controller indirectly through modification of the error feedback signal (via X). This antiwindup approach introduces an observer structure into the controller, as seen by substituting (2) for u_c in (1):

$$\dot{x} = (A - \Lambda C)x + (B - \Lambda D)e + \Lambda u_a \tag{3}$$

With this view, the antiwindup design problem reduces to determining a suitable choice for Λ. Specifically, one possible goal of antiwindup design is to choose Λ to make the above dynamics relatively fast and well damped in order to regulate to zero any differences between the limited actuator signals, u_a, and the actuator signals commanded by the controller, u_c. This is a more general statement of the tracking mode.

Currently, optimal methods of determining Λ with respect to system stability and the tracking mode do not exist. However, two particular selections for Λ which have been used successfully in practice are now discussed.

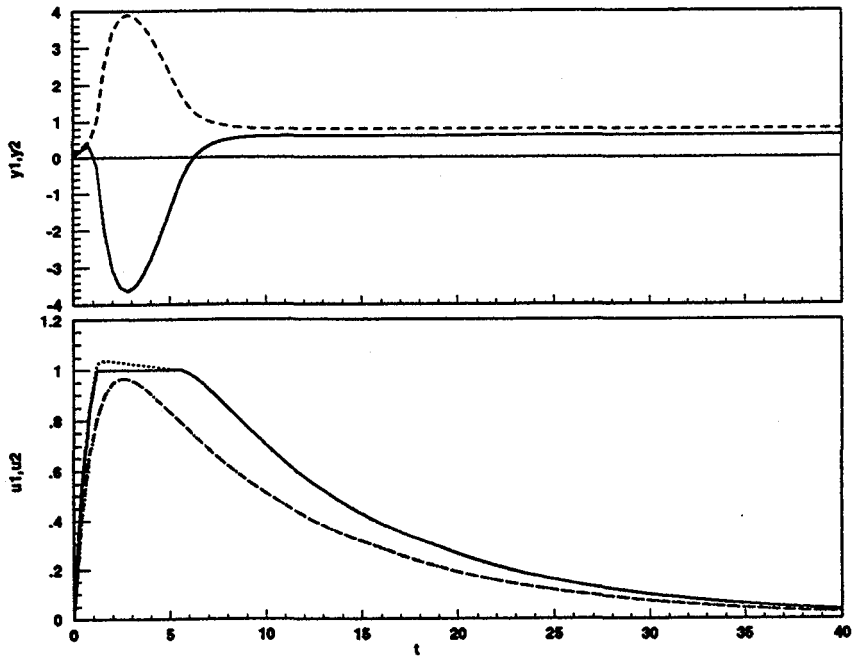

Figure 12: System M1 step response using decoupled antiwindup method

2.2.1 Decoupled MIMO Tracking Mode

An antiwindup method which is commonly used [DSE87], [Mat93], is a generalization of the tracking mode concept of Section 2.1 to the MIMO case. Consider the augmented controller description (1) -(2), with $D = 0$. In order to implement a tracking mode, the actuator error term in (1), $\Lambda(u_a - u_c)$, must correspond to the state error which, when driven to zero, will yield a controller output corresponding to the limited control vector, u_a. To achieve this, first define the "desired" state, x_d, as a controller state satisfying

$$u_a = Cx_d,$$

i.e., x_d is the state that the controller would need to be in so that $u_c = u_a$. Using the above expression with (2), the actuator error can now be expressed as

$$u_a - u_c = C(x_d - x).$$

Therefore, the state error, $(x_d - x)$, will drive the antiwindup system (1) if Λ is chosen such that:

$$\Lambda C = kI, \tag{4}$$

so that $\Lambda(u_a - u_c) = kI(x_d - x)$, where k is a scalar constant, and a (left) inverse of C exists. This choice for Λ effectively back calculates the appropriate state error given the actuator error, and multiplies it by a scalar gain in order to dominate the plant feedback error term, Be.

Application of the above scheme to system M1, with $k = 10$, is shown in Figure 12. Note that, in comparison to the responses shown in Figure 5, some, but not all, of the adverse effects of the limits have been eliminated in the plant output response. Note also the decoupled nature of this windup scheme, where tracking is imposed on u_1, and the nonlimited actuator, u_2, is not affected.

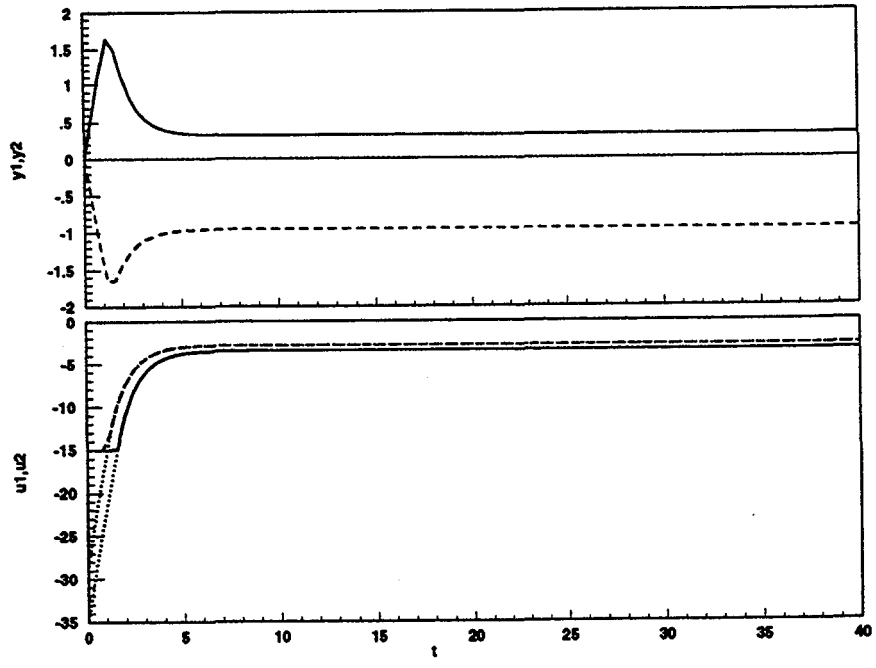

Figure 13: System M2 step response using Hanus' antiwindup method

2.2.2 Hanus' Method

As seen in Sections 2.1 and 2.2.1, windup can be alleviated by introducing a tracking mode if and only if limited conditions exist. This is accomplished in the CAW approach with the static matrix gain, X, chosen such that the actuator error (inner loop) dominates the plant feedback error (outer loop) in the system of Figure 9, and in the decoupled method of Section 2.2.1 by choosing Λ such that $\Lambda C(x_d - x) = kI(x_d - x)$ dominates Be.

In the case when K has a D matrix which is (left) invertible, it can be seen from (3) that while actuators are limited, the effect of the erroneous outer loop feedback, e, can be *eliminated* by choosing Λ such that:

$$\Lambda D = B.$$

The above choice for Λ renders the states of the controller uncontrollable from the e input, and therefore no windup will occur. This antiwindup strategy was first developed in [HKH87], however, the above view of the method is given in [CM90].

Figure 13 illustrates the application of the Hanus antiwindup technique to system M2. The plant output response depicts the elimination of *some* of the adverse behavior when compared to that of Figure 7. Specifically, the long-term overcorrection has been eliminated. However, the more significant initial overshoot is still present. This is due, as in the decoupled method, to the manner in which the nonlimited actuator, u_2, is being treated. This issue will be addressed in Section 3. It is interesting to note that this method does not force the control signals to approach their limited values any faster, as in the tracking mode approaches. It instead uses the difference $(u_a - u_c)$ to prevent the discrepancy between the control signals and plant input from affecting the controller states.

A few comparisons should be made here regarding the antiwindup methods presented. Recall that the Hanus technique requires the controller realization to contain a D matrix which is (left) invertible. However,

in the decoupled and CAW techniques, difficulties may arise when $D \neq 0$. In particular, for the decoupled method, where Λ is chosen as in (4), it is desired that the limit feedback, u_a, dominate the tracking error feedback, e, in (3). This cannot be guaranteed if $D \neq 0$, because the feedback error term, $(B - \Lambda D)e$, will depend on Λ. For the CAW approach, $D \neq 0$ will produce an algebraic loop in the implementation shown in Figure 9. Although alternative implementations can be obtained to alleviate this problem, it is shown in [CMN89] that the resulting system is very sensitive to measurement noise in u_a, and exhibits stability problems for non-minimum phase controllers. These issues illustrate that the existence of a controller direct-feedthrough term is an important consideration in determining which antiwindup method is best suited for a given application.

3 Directionality

As defined in the previous section, the windup problem is due to inconsistency between the controller output, u_c, and the effective plant input, u_a. The MIMO examples illustrate that the goal of graceful performance degradation is in general not achieved solely by eliminating windup effects. To further illustrate this point, consider again system M1, where the responses obtained by implementing the MIMO tracking mode approach of Section 2.2.1 are shown in Figure 12. An alternative approach to the windup problem is to implement the CAW method, where the parameter X is now a "large" matrix-valued constant. Choosing X such that its first column is $[100\ 100]^T$ (the second column does not affect the system, since u_2 never exceeds its limit) yields the responses shown in Figure 14. Note that *all* adverse effects in the output signals due to saturation have been significantly reduced. Comparison of Figures 14 and 12 shows that while both antiwindup methods achieve a tracking mode for the limited actuator, $u_{c,1}$, they differ in how they treat the ***nonlimited*** actuator, $u_{c,2}$. Viewing this situation geometrically, it can be said here that the CAW method ***maintains the control direction.*** In other words, the CAW approach restricts the nonlimited actuator in a similar manner as it does the limited actuator, wheras the decoupled method changes the control direction by only affecting the limited actuator. The reason that this has a large effect in performance is because in MIMO systems, the plant gain is a function of its input direction. Since the saturation nonlinearity operates independently on each actuator, it can change both properties of the control signal. This is especially problematic when the plant has a high condition number, since its gain varies widely with respect to its input direction. Therefore, in the MIMO limit problem, care must be taken to ensure that the effective actuator signal, u_a, does not produce adverse side-effects due to its direction.

Note that for the above example, no specific method is employed to generate the appropriate CAW matrix gain, X. In general, a linear antiwindup design approach which takes into account directionality issues is not available and is a current research issue. The optimality issues involved in such a problem are described in [CMN89]. However, this problem has been addressed in the context of the Hanus antiwindup method by the introduction of an additional nonlinearity into the system, which modifies u_c such that u_a and u_c have the same direction [CM90]. This technique is now described and illustrated via system M2, in the context of the Hanus antiwindup scheme. This system will be referred to in the sequel as system M2H.

3.1 Scalar Projection (SP)

A typical characteristic of controllers with significant direct feedthrough (D) terms is that limits tend to be reached immediately in response to sufficiently large step commands. This behavior is seen in the limited M2 response of Figure 7. Also note that the control commands taper off as the plant outputs approach the

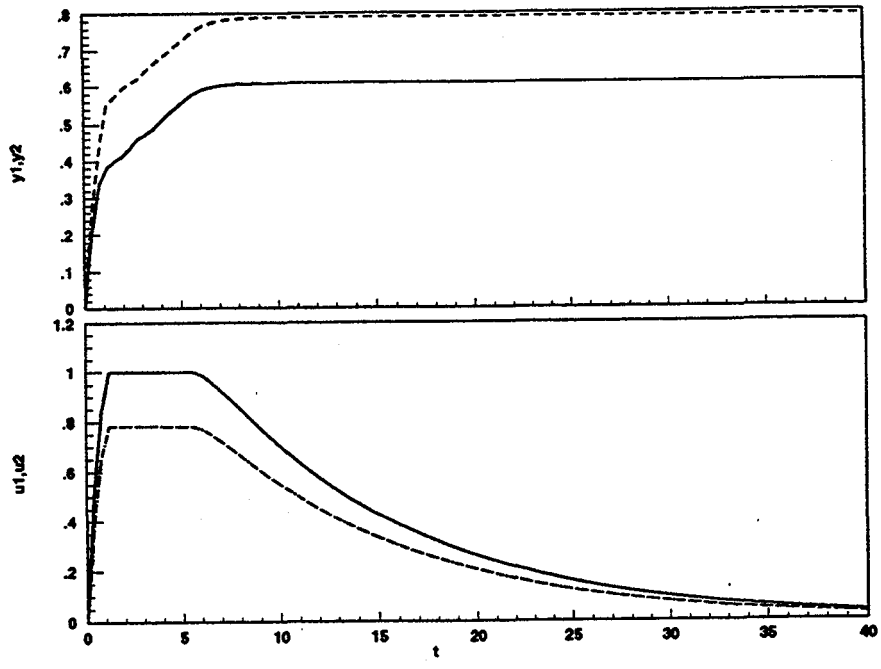

Figure 14: System M1 CAW step response

reference command. This can be illustrated more generally by considering a nominal system with n reference commands having a proper controller and a strictly proper plant. The control signal, $u = u_c = u_a$, resulting from a step reference input $\frac{1}{s}k$, where $k = [k_1\ k_2\ \ldots\ k_n]^T$ is

$$u(s) = K(I + PK)^{-1}\frac{1}{s}k.$$

Application of the initial-value theorem yields:

$$\begin{aligned} u(0) &= \lim_{s\to\infty} su(s) \\ &= \lim_{s\to\infty} K(I + PK)^{-1}k \\ &= \lim_{s\to\infty} Kk \\ &= \lim_{s\to\infty} [C(sI - A)^{-1}B + D]k, \end{aligned}$$

where (A, B, C, D) is the state space realization of the controller. Thus the initial control command, $u(0)$, is determined by:

$$u(0) = Dk. \tag{5}$$

The point here is that the initial control command depends only on the controller structure and reference input, and is not affected by either the plant or the saturation nonlinearity. Thus, with the knowledge of the desired nominal control command, it seems advantageous to modify this signal in such a way that the resulting command maintains the original control direction but does not violate any limits. This is desirable because preserving the original direction of u_c will preserve the plant gain, thus in a sense maintaining the nominal closed-loop characteristics. This can be achieved by introducing a nonlinear map, $N : u_c \mapsto \hat{u}$, into the antiwindup system, as shown in Figure 15. A simple nonlinearity, suggested in [CMN89], which possesses

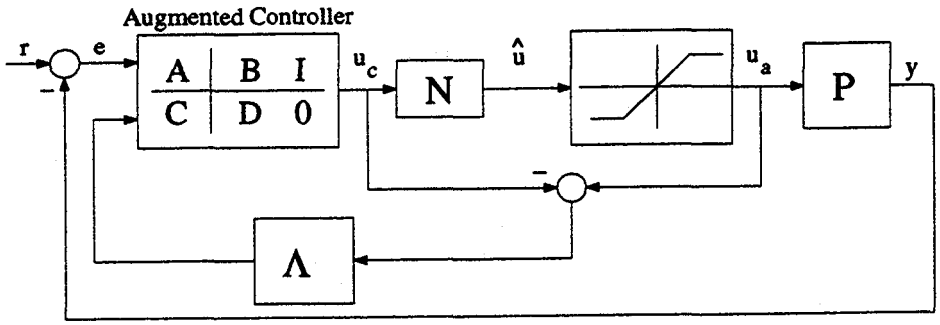

Figure 15: Nonlinear modification of controller output

the desired modification properties is now described. First define the following matrix of limit values:

$$L = \mathrm{diag}(L_1, L_2, \ldots, L_m), \tag{6}$$

where L_i is the saturation limit value for the i'th actuator, and m is the number of actuators. A limit-normalized control signal, $\tilde{u}$, is now defined as:

$$\tilde{u} = L^{-1} u_c,$$

so that a limit condition exists if and only if $\tilde{u}_i > 1$, $i = 1 \ldots m$. The appropriate direction-preserving nonlinearity is simply a scalar multiple of the nominal control signal, which yields the modified control command, $\hat{u}$, as follows:

$$\hat{u}(t) = N(u_c) = \alpha[\tilde{u}(t)] u_c(t), \tag{7}$$

where

$$\alpha[\tilde{u}(t)] = \frac{1}{\max_i(1, \tilde{u}_i(t))}.$$

As noted in [CM90], this operation on u_c effectively *replaces* the saturation element with the scalar multiplier α. This is because α is chosen above such that no component of $\hat{u}$ will exceed its limit. The saturation will therefore be operating as an identity operator, and $u_a = \hat{u}$. The performance of system M2H with this modification is shown in Figure 16. Note the large initial overshoot has been eliminated, and all signals are well-behaved.

An interesting point that this procedure illustrates is that, in the absence of a single antiwindup design procedure encorporating both antiwindup and directionality specifications, it is plausible to treat the antiwindup and directionality issues independently. This is due to the fact that the antiwindup methods considered here only depend on the difference $(u_a - u_c)$, not on the specific nature of the nonlinearity. Thus windup effects are eliminated *regardless* of the nonlinearity, justifying the "replacement" of the saturation operator with the operator N, which is more favorable with respect to directionality. It is this concept which motivates an alternative choice of N to further improve performance. This is the topic of the next two sections.

3.2 Optimal Projection (OP)

To motivate an improvement to the scalar projection method, it is helpful to consider a geometric view of the directionality problem. Specifically, consider the following scenario for the two-actuator system M2H. Figure 17 depicts the actuator space, where the directional nature of the plant gain is shown explicitly via

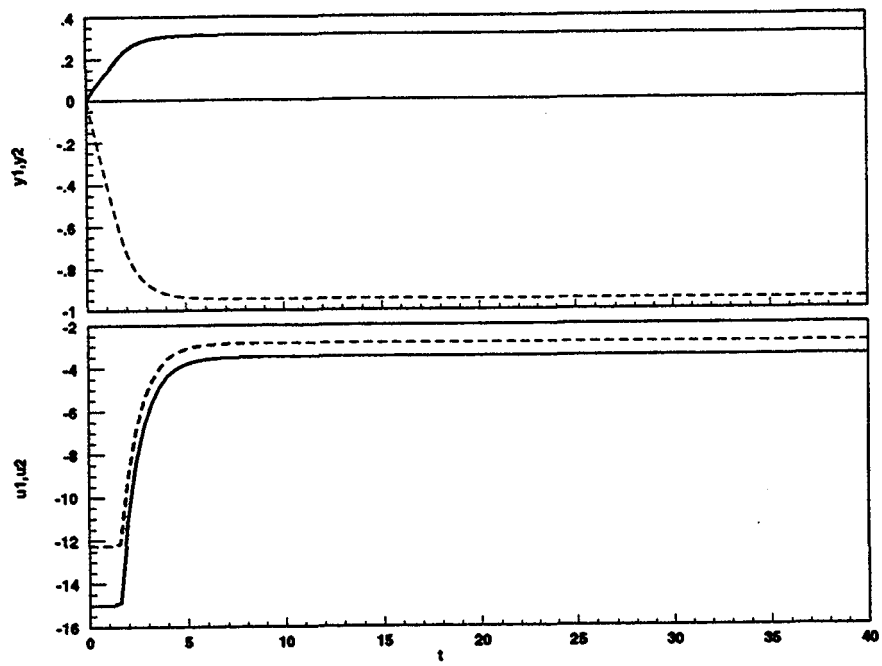

Figure 16: System M2H step response using SP directionality compensation

the plant input principal directions, $\overline{u}$ and $\underline{u}$, corresponding to the maximum and minimum singular values, respectively. The limits are shown by the dotted lines. An initial control command, u_c, is shown which violates the limits. In the absence of directionality compensation, the command $u_a = \text{sat}(u_c)$ will be given to the plant. Since this signal has a direction different from that of u_c, the resulting plant output may be quite different from the nominal case. The Hanus antiwindup scheme will prevent the resulting erroneous feedback, e, from affecting the controller states. However, Figure 13 illustrates that the signal itself may be entirely unacceptable, with respect to reference-tracking requirements, as evidenced by the amount of overshoot.

A useful alternative view of the above situation is obtained by modeling the saturation nonlinearity as a plant input disturbance, as done in the beginning of Section 2. The effective plant actuator command is thus represented as:

$$u_a = u_c - d,$$

and the resulting plant output is:

$$y = Pu_c - Pd. \tag{8}$$

A key observation here is that the effect of the disturbance will be large if d has a significant component in the $\overline{u}$-direction. This is in fact the case when no directionality compensation is used (i.e. when $u_a = \text{sat}(u_c)$), where it is easily verified that $d = u_a - u_c$ can have such a component. The scalar projection method improves the plant output response by modifying the control command so that $u_a = \hat{u}$ in Figure 17, where $\hat{u} = \alpha u_c$, with α is defined as in (7). This yields a plant output of:

$$y = P\hat{u} = \alpha P u_c, \tag{9}$$

which is simply a *scalar multiple* of the nominal output. Thus directionality effects are eliminated. An alternative approach, suggested in [CM90], is to actually use the directional characteristics of the plant to

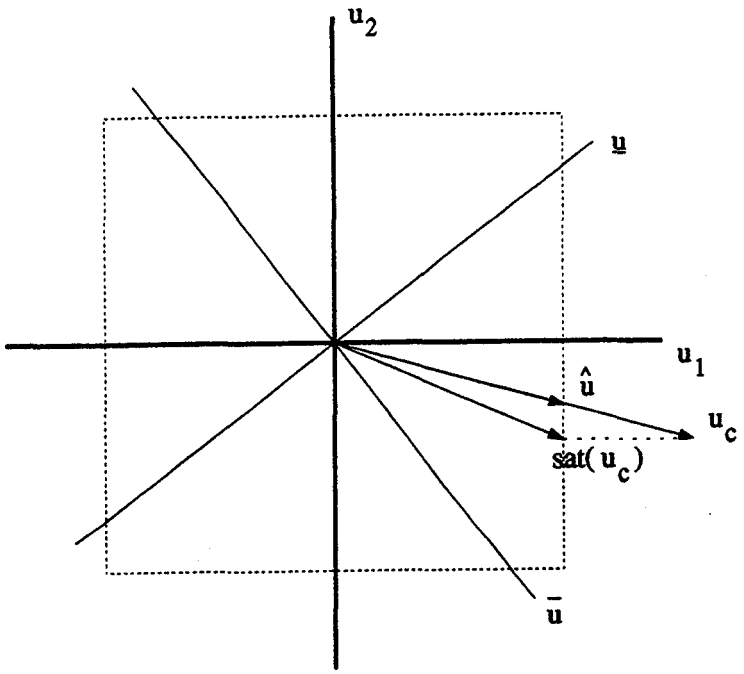

Figure 17: Geometric view of saturation and SP compensation effects on the controller output

modify u_c such that d is optimal with respect to its effect on the plant output, Pd. To a first approximation, this will be accomplished if d is in the $\underline{u}$-direction, i.e., $d = \gamma \underline{u}$, with γ a scalar. This yields the following plant output contribution of the disturbance:

$$y_d \triangleq Pd = \gamma P\underline{u} = \gamma \underline{\sigma} \underline{y}, \tag{10}$$

where $\underline{y}$ is the output principal direction corresponding to input principal direction $\underline{u}$, and $\underline{\sigma}$ is the minimum singular value. Geometrically, this corresponds to the situation shown in Figure 18, where the modified control command, $\hat{u}$, is obtained from the original command, u_c, by a projection in the $\underline{u}$-direction onto the closest point in the actuator space which does not violate any limits. Note that for the scalar projection method, (8) and (9) imply:

$$y_d = Pu_c - y = (1 - \alpha)Pu_c,$$

which depends on the original control direction, and thus in general performance will still be affected by plant directionality. An attractive feature of (10) is that the gain of d through P will always be as small as possible, regardless of the control direction. Therefore, one would expect the resulting system performance using this approach to possess even less adverse effects due to plant directionality than scalar projection.

The projection concept is now made more precise by viewing the choice of d as an optimization problem. Specifically, consider the problem of determining the optimal value, d^*, such that its contribution to the plant output, y_{d^*}, is as small as possible. A resulting optimally modified control command, $\hat{u}^*$, is then determined from:

$$\hat{u}^* = u_c - d^*. \tag{11}$$

The following optimization problem will accomplish this goal:

$$\min_d ||y_d||^2, \tag{12}$$

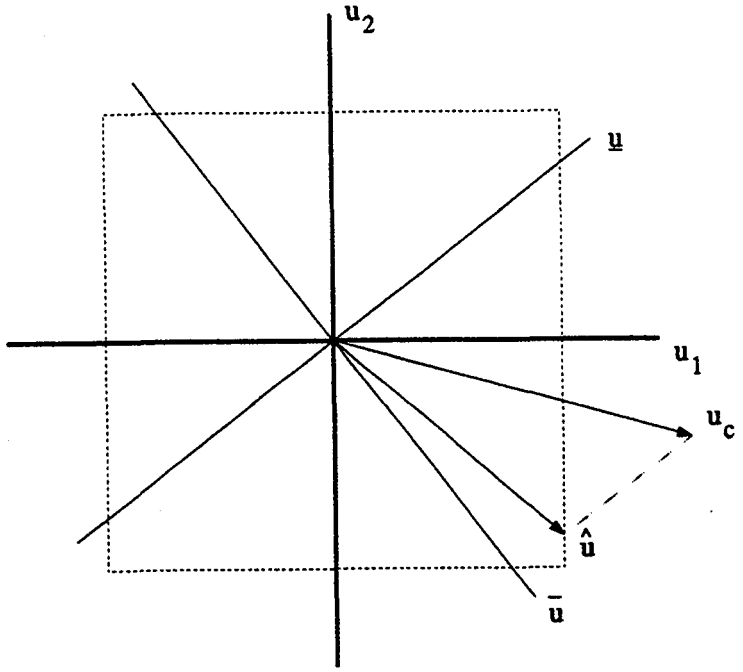

Figure 18: Projection of the controller output in the $\underline{u}$-direction

Subject to:

$$L^{-1}[u_c(t) - d(t)] \leq \mathbf{1}, \tag{13}$$

where L is defined as in (6), and $\mathbf{1}$ is an m-dimensional vector with all of its components equal to one.

This concept is now illustrated for the case of a two-actuator plant. Let d be a disturbance, having the following representation with respect to the plant input principal directions:

$$d = \gamma\,\underline{u} + \beta\,\overline{u}, \tag{14}$$

where γ and β are scalars. Since $\underline{u}$ and $\overline{u}$ form an orthonormal basis, this is simply a coordinate change from the standard basis, $\{e_1\ e_2\}$ to $\{\underline{u}\ \overline{u}\}$, where γ and β are the coordinates in the new system. Using (14), y_d can be expressed as

$$y_d = Pd = P(\gamma\,\underline{u} + \beta\,\overline{u}) = \gamma\,\underline{\sigma}\,\underline{y} + \beta\,\overline{\sigma}\,\overline{y}. \tag{15}$$

To obtain the constraint equation, consider the case where one limit is in effect at a time. This reduces (13) to:

$$u_l - \gamma\,\underline{u}_l - \beta\,\overline{u}_l = L_l, \tag{16}$$

where the "l" subscript represents the index of the limited component of u_c. The "c" subscript has been dropped to simplify notation. Substituting (15) and (16) into (12) and (13) yields the following optimization problem, for the case when $m = 2$:

$$\min_{\gamma,\beta}\{\gamma^2\,\underline{\sigma}^2 + \beta^2\,\overline{\sigma}^2\}, \tag{17}$$

Subject to:

$$u_l - \gamma\,\underline{u}_l - \beta\,\overline{u}_l = L. \tag{18}$$

From (18), the optimal value of the limited actuator, u_l, is immediately obtained as:

$$\hat{u}_l^* = L_l. \tag{19}$$

The optimization is now solved by eliminating β using the constraint equation (18), substituting into (17), and minimizing the resulting function with respect to the single scalar variable, γ. This process yields the optimal value of γ to be:

$$\gamma^* = \frac{ABK^2}{B^2K^2 + 1},$$

where $K = \overline{\sigma}/\underline{\sigma}$, the condition number of the plant, and

$$\begin{aligned} A &= \frac{u_l - L}{\overline{u}_l}, \\ B &= \frac{\underline{u}_l}{\overline{u}_l}. \end{aligned}$$

The desired optimal value, d_{nl}^* — the subscript "nl" represents the index of the *nonlimited* actuator component — is obtained by substituting γ^* and β^* into the nl'th component of (14). Finally, substituting the result into (11) yields an expression for the optimally modified nonlimited control command:

$$\hat{u}_{nl}^* = u_{nl} - \frac{A(BK^2\underline{u}_{nl} - \overline{u}_{nl})}{(B^2K^2 - 1)} \tag{20}$$

Figure 19 compares the step response and control signals for system M2H using the above directionality compensation scheme (solid line) with that obtained using the scalar projection approach (dashed line). The optimal projection (OP) method is seen to yield faster step response when limits are in effect. In fact the y_1 response is actually faster than that of the nominal design (Figure 6). This is due to the fact that (20) uses only open loop plant information, and thus performance is limited only by the physical plant capability. In other words, the closed loop design does not affect limited performance. The actuator signals illustrate specifically how conservatism is reduced when using (20) to calculate the optimal value of the nonlimited actuator.

3.3 Combined Scalar Projection and Optimal Projection

The OP directionality compensation scheme is seen in the previous section to yield superior performance compared with SP. Unfortunately, it does not always exhibit such behavior. This is illustrated in Figure 20, where a reference input of $r_3 = [0.122 \ -0.992]^T$ has been used. This reference command differs only in direction to the previously applied r_2. Note that for convenience, all reference inputs have been chosen such that $||r_i|| = 1, i = 1, 2, 3$. The OP method is seen to produce significant overshoot in y_1, while the SP method performs exactly as it did using the previous reference input. This indicates that each method has desirable properties. A directionality compensation scheme containing elements of each method is now proposed.

To address this problem, it must first be determined what is causing the adverse behavior of OP. Consider the alternative view of the nominal system shown in Figure 21, where the saturation nonlinearity is modeled by the plant input uncertainty $\Delta = \text{diag}(\delta_1, \delta_2, \ldots, \delta_m)$, where $|\delta_i| < 1$. It is well known that in MIMO systems, performance can suffer greatly in the presence of such uncertainties. This issue is now investigated via the classical notion of logarithmic sensitivity, generalized to the MIMO case by considering the first order change of a desired transfer function with respect to the system perturbation [BB91]. For the present case,

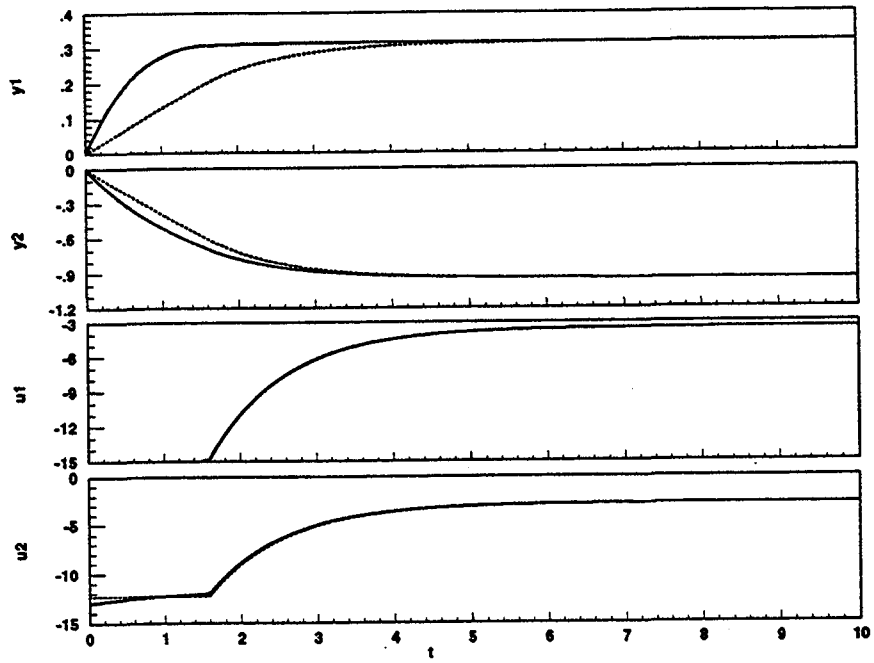

Figure 19: System M2H step response comparison of OP and SP for $r = r_2$

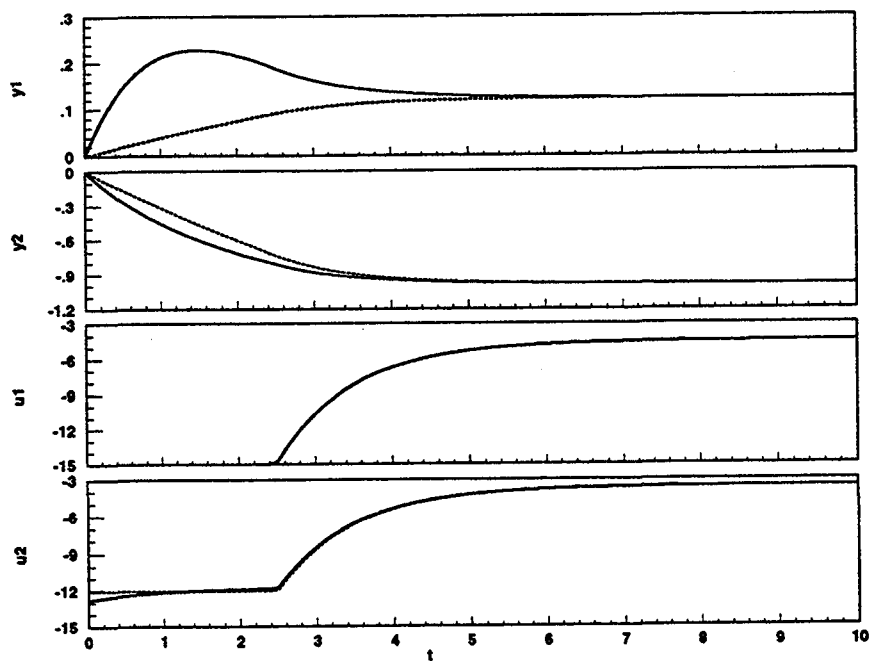

Figure 20: System M2H step response comparison of OP and SP for $r = r_3$

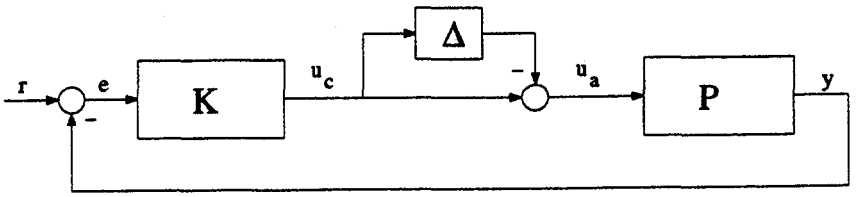

Figure 21: Nominal system with plant input uncertainty

the transfer function of interest is that from the reference input to the tracking error, H_{er}. The system perturbation, Δ, yields the perturbed plant $\tilde{P} = P(I - \Delta)$. The perturbed transfer function, $\tilde{H}_{er}$, is:

$$\tilde{H}_{er} = [I + P(I - \Delta)K]^{-1} = [I + PK - P\Delta K]^{-1}$$

Applying the matrix inversion lemma yields:

$$\tilde{H}_{er} = (I + PK)^{-1} + (I + PK)^{-1}P\Delta\underbrace{(I - K(I + PK)^{-1}P\Delta)^{-1}}K(I + PK)^{-1}, \tag{21}$$

Note that the first term above is simply the nominal transfer function H_{er}. The MIMO sensitivity function, δH_{er}, is determined by computing the first order representation of the second term with respect to Δ. This can be obtained via one further application of the matrix inversion lemma to the bracketed term above:

$$(I - K(I + PK)^{-1}P\Delta)^{-1} = I + K(I + PK - P\Delta K)P\Delta.$$

Substituting the above identity into (21), and retaining only first order terms in Δ yields the desired first order change in H_{er}:

$$\delta H_{er} = (I + PK)^{-1}P\Delta K(I + PK)^{-1} = H_{ed}\Delta H_{er}, \tag{22}$$

where H_{er} and H_{ed} are the closed loop transfer functions for the nominal system shown in Figure 8, from the reference and disturbance inputs, respectively, to the tracking error.

A comparison between the SP and OP directionality compensation schemes from a sensitivity point of view for a two-actuator system will now be made by determining an equivalent Δ perturbation yielded by each scheme, Δ_{SP} and Δ_{OP}. This is obtained from the relationship

$$u_a = (I - \Delta)u_c, \tag{23}$$

using either (7), or (19) and (20), to determine $\hat{u} = u_a$. For the SP algorithm, $u_a = \alpha u_c$ is therefore substituted into (23), yielding:

$$\Delta_{SP} = (1 - \alpha)I = \left(1 - \frac{L_l}{u_{c,l}}\right) I \triangleq \delta I, \tag{24}$$

where the "l" subscript represents the index of the limited actuator, as in Section 3.2. To repeat this process for the OP method, individual components must be considered. From (19):

$$u_{a,l} = \hat{u}_l^* = L_l = (1 - \delta_l)u_{c,l} \tag{25}$$

where $\delta_l = 1 - L_l/u_{c,l}$ is identical to that of the SP method. Considering the nl'th component of (11) yields:

$$u_{a,nl} = \hat{u}_{nl}^* = u_{c,nl} - d_{nl}^* = (1 - \delta_{nl})u_{c,nl} \tag{26}$$

where $\delta_{nl} = d^*_{nl}/u_{c,nl}$, and (the negative of) d^*_{nl} is given by the second term in (20).

The above establishes that for SP, $\Delta = \Delta_{SP} = \delta I$, while in OP, $\Delta = \Delta_{OP} = \text{diag}(\delta_1, \delta_2)$. Since $\{\Delta_{SP}\} \subset \{\Delta_{OP}\}$, (22) implies that a wider range of closed loop behavior is expected from the OP scheme. This is analogous to comparing robust stability and performance measures obtained using singular values, where $\Delta \in \mathbf{R}^{m \times m}$, with those obtained using structured singular values, where $\Delta \in \text{diag}(\delta_1, \delta_2, \ldots, \delta_m)$. These concepts illustrate that performance and stability properties suffer as Δ becomes more general. This property can be seen in (22) because for SP, the effect of Δ is simply to multiply the product of two nominal closed loop quantities by a scalar, since for $\Delta = \Delta_{SP}$, (22) reduces to $\delta H_{er} = k H_{ed} H_{er}$. For OP, however, system directionality will have an effect on the closed loop performance, due to the distinct diagonal elements of Δ_{OP}. It is this characteristic that leads to *both* the superior and inferior performance of OP compared with SP, observed in Figures 19 and 20.

To apply the above ideas in a quantitative manner, it is necessary to determine appropriate bounds on Δ_{SP} and Δ_{OP}. Recall from the discussion at the beginning of Section 3.1 that $\max_t |u_c(t)| = u_c(0)$, where $u_c(0)$ is given by (5). Therefore, the desired Δ_{SP} and Δ_{OP} can be obtained from (24)-(26) with $u_c = u_c(0)$. Since $u_c(0)$ is a function of the reference input, so must be Δ. Furthermore, the limit L_l appears as a parameter. Thus $\Delta = \Delta(r; L_l)$, and the sensitivity function (22) can now be evaluated for any reference input. It is of particular interest to examine the singular value decomposition of (22), because this will provide the sensitivity magnitude variation, as well as explicit reference input directions yielding such magnitudes. This is illustrated in Figure 22 for $r = r_3$, where the singular values of (22) are shown for both directionality schemes. Specifically, the solid line represents both the maximum and minimum singular values when $\Delta = \Delta_{SP}(r_3; 15)$, while the dashed lines represent those for the case when $\Delta = \Delta_{OP}(r_3; 15)$. This is significant because Figure 22 implies that from the sensitivity point of view, there exists reference directions for which OP is superior to SP (as expected from Figure 19), and other directions for which OP performs worse (as in Figure 20). Specific reference directions which produce such behavior are given by $\underline{u}(\delta H_{er})$ and $\overline{u}(\delta H_{er})$, the singular vectors corresponding to the minimum and maximum singular values of (22). This suggests the parameterization of the map $N : u_c \mapsto \hat{u}$ shown in Figure (15) by the reference input, r. In other words, it would be desirable if $\hat{u} = N(u_c; r)$, so that sensitivity considerations can determine which nonlinearity is applied.

Note that in the above discussion, the analysis provides reference directions which yield the maximum and minimum possible sensitivities for the OP scheme when $\Delta = \Delta(r_3; L_l)$. This is not entirely meaningful, since application of these reference directions to the system produces $\Delta = \Delta(\underline{u}(\delta H_{er}); L_l)$, or $\Delta = \Delta(\overline{u}(\delta H_{er}); L_l)$. It is of greater interest to obtain such directions which are consistent with the Δ used to generate them. To this end, an iterative scheme is formulated:

Step 0: Choose a reference input magnitude, M, and initial direction, $\tilde{r}_0$.

Step 1: Calculate $\Delta_{OP}(M\tilde{r}_i; L_l)$ from (25)-(26).

Step 2: Perform the singular value decomposition of (22) with $\Delta = \Delta_{OP}$.

Step 3: Set $\tilde{r}_{i+1} = \overline{u}(\delta H_{er})$.

Step 4: If $||\tilde{r}_{i+1} - \tilde{r}_i|| < \epsilon$, for some $\epsilon > 0$, stop. Otherwise, return to Step 1.

By repetitively using $M\tilde{r}_i$ to generate Δ, one would expect the resulting $\tilde{r}_{i+1} = \overline{u}(\delta H_{er})$ to approach $\tilde{r}_i$, providing the desired consistency between Δ and $\overline{u}(\delta H_{er})$. While convergence is observed, it takes place in a somewhat unexpected manner. Instead of converging as described in Step 4 above, the iteration converges

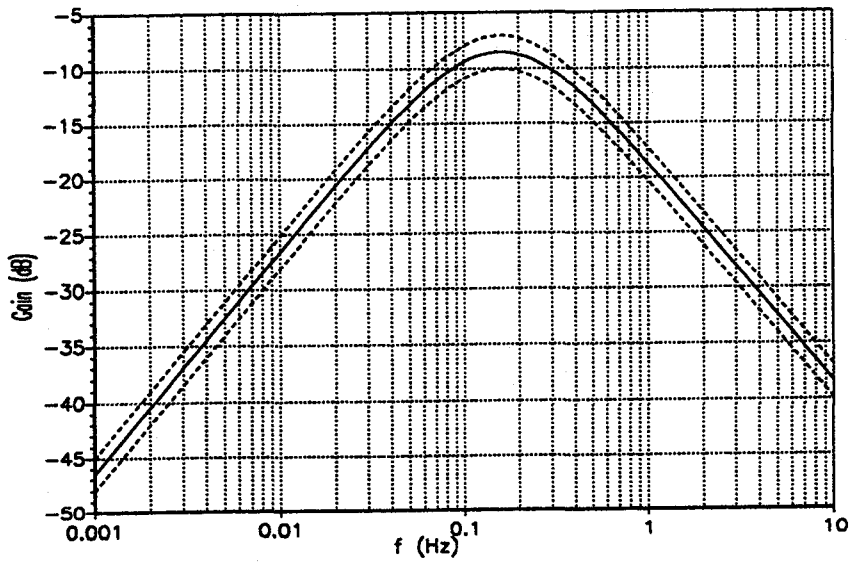

Figure 22: Singular values of δH_{er} for SP and OP directionality compensation schemes

such that $||\tilde{r}_{i+1} - \tilde{r}_{i-1}|| < \epsilon$. In other words, convergence was observed among every other $\tilde{r}$ in the iteration. This yields *two* pairs of singular vectors: $\overline{u}_i(\delta H_{er})$, $\underline{u}_i(\delta H_{er})$, $i = 1, 2$. These directions are shown in Figure 23 to partition the reference input space into regions R_I, R_{II}, and R_{III}. With respect to these regions the following nonlinear map $N : u_c \mapsto \hat{u}$ is proposed:

$$\hat{u} = N(u_c; r) = \begin{cases} \alpha u_c & , r \in R_I \\ \hat{u}^* & , r \in R_{II} \\ \lambda \alpha u_c + (1-\lambda)\hat{u}^* & , r \in R_{III} \end{cases},$$

where α is from (7), $\hat{u}^*$ is from (19)-(20), and $0 \leq \lambda \leq 1$. The well-behaved response of M2H shown in Figure 19 results from using OP with $r_2 \in R_{II}$, while the poor response shown in Figure 20 results from using OP with $r_3 \in R_{III}$. To improve performance for the input r_3, the convex combination of the SP and OP methods suggested above is implemented, using $\lambda = 0.8$. The performance of M2H using this approach is compared with that of the SP scheme ($\lambda = 1$) in Figure 24, where the overshoot seen in Figure 20 due to OP has been eliminated, while improving upon the conservatism of SP.

4 Conclusion

This work has investigated the problem of saturating actuators in MIMO systems. It is seen that the directional nature of such systems introduces significant degradation in closed-loop performance, in addition to controller windup. A directionality compensation technique is developed here which uses knowledge of the plant input principal directions and condition number to provide potentially less conservative controls than the conventional strategy of maintaining the control direction. However, the reduced conservatism does not always result in improved performance. The concept of MIMO sensitivity is employed as an indicator of which scheme should be used — or how the two schemes can be combined — to result in the best overall closed loop performance.

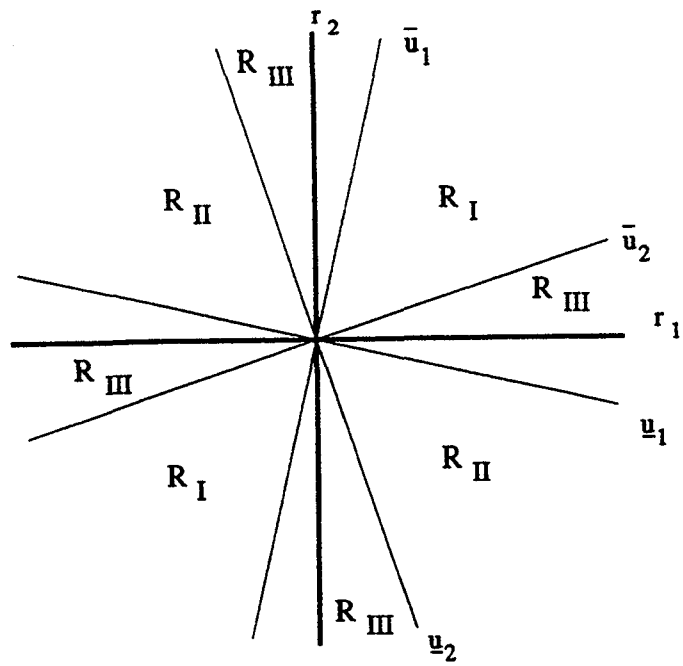

Figure 23: Reference input space partitioning effect of iterative scheme

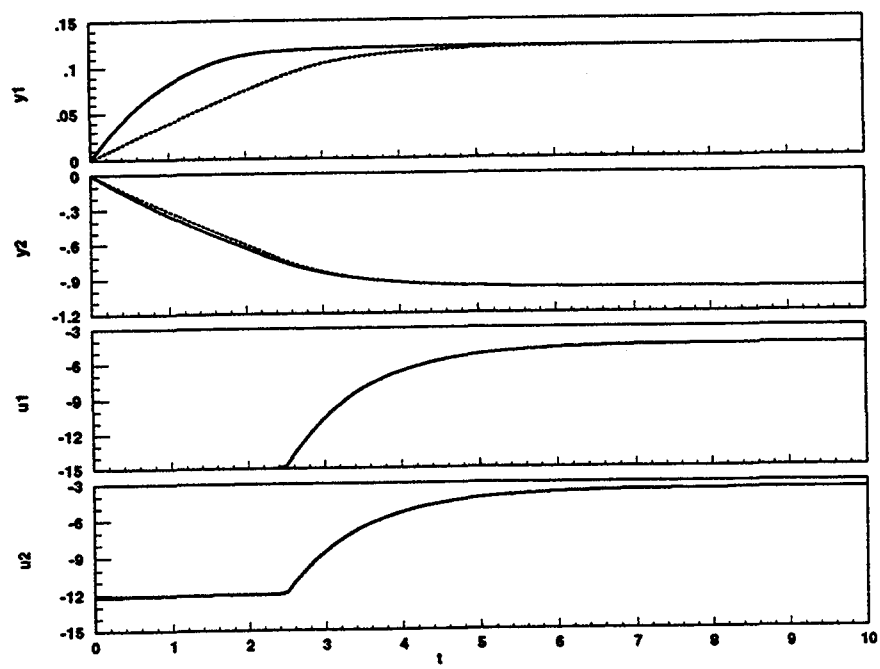

Figure 24: System M2H step response comparison of combined OP-SP and SP directionality compensation techniques for $r = r_3$

References

[BB91] S. P. Boyd and C. H. Barratt. *Linear Control Design: Limits of Performance.* Prentice-Hall, Englewood Cliffs, NJ, 1991.

[CM90] P. J. Campo and M. Morari. Robust control of processes subject to saturation nonlinearities. *Computers chem. Engng.*, 14(4/5):343–358, 1990.

[CMN89] P. J. Campo, M. Morari, and C. N. Nett. Multivariable anti-windup and bumpless transfer: A general theory. In *Proc. 1989 Am. Control Conf.*, pages 1706–1711, 1989.

[DSE87] J. C. Doyle, R. S. Smith, and D. F. Enns. Control of plants with input saturation nonlinearities. In *Proc. 1989 Am. Control Conf.*, pages 1034–1039, 1987.

[HKH87] R. Hanus, M. Kinnaert, and J. L. Henrotte. Conditioning technique, a general anti-windup and bumpless transfer method. *Automatica*, 23:729–739, 1987.

[Mat93] D. Mattern. A comparison of two multi-variable integrator windup protection schemes. In *Proc. AIAA Guidance, Navigation and Control Conf.*, pages 1012–1020, 1993.

REPORT DOCUMENTATION PAGE

Form Approved
OMB No. 0704-0188

1. AGENCY USE ONLY (*Leave blank*)	2. REPORT DATE	3. REPORT TYPE AND DATES COVERED
	April 1994	Final Contractor Report

4. TITLE AND SUBTITLE

Control Strategies for Systems With Limited Actuators

5. FUNDING NUMBERS

WU–505–62–50
G–NAG3–1232

6. AUTHOR(S)

Vincent R. Marcopoli and Stephen M. Phillips

7. PERFORMING ORGANIZATION NAME(S) AND ADDRESS(ES)

Case Western Reserve University
Department of Electrical Engineering and Applied Physics
Cleveland, Ohio 44106

8. PERFORMING ORGANIZATION REPORT NUMBER

E–8714

9. SPONSORING/MONITORING AGENCY NAME(S) AND ADDRESS(ES)

National Aeronautics and Space Administration
Lewis Research Center
Cleveland, Ohio 44135–3191

10. SPONSORING/MONITORING AGENCY REPORT NUMBER

NASA CR–195307

11. SUPPLEMENTARY NOTES

Project Manager, Walt Merrill, Instrumentation and Control Technology Division, organization code 2550, NASA Lewis Research Center, (216) 433–6328.

12a. DISTRIBUTION/AVAILABILITY STATEMENT

Unclassified - Unlimited
Subject Category 07

12b. DISTRIBUTION CODE

13. ABSTRACT ***(Maximum 200 words)***

This work investigates the effects of actuator saturation in multi-input, multi-output (MIMO) control systems. The adverse system behavior introduced by the saturation nonlinearity is viewed here as resulting from two mechanisms: 1) Controller windup - a problem caused by the discrepancy between the limited actuator commands and the corresponding control signals, and 2) Directionality - the problem of how to use nonlimited actuators when a limited condition exists. The tracking mode and Hanus methods are two common strategies for dealing with the windup problem. It is seen that while these methods alleviate windup, performance problems remain due to plant directionality. Through high gain conventional antiwindup as well as more general linear methods have the potential to address both windup and directionality, no systematic design method for these schemes has emerged; most approaches used in practice are application driven. An alternative method of addressing the directionality problem is presented which involves the introduction of a control direction preserving nonlinearity to the Hanus antiwindup system. A nonlinearity is subsequently proposed which reduces the conservation inherent in the former direction-preserving approach, improving performance. The concept of multivariable sensitivity is seen to play a key role in the success of the new method.

14. SUBJECT TERMS	15. NUMBER OF PAGES
Feedback control; Contacts; Actuator limits	28
	16. PRICE CODE: A03

17. SECURITY CLASSIFICATION OF REPORT	18. SECURITY CLASSIFICATION OF THIS PAGE	19. SECURITY CLASSIFICATION OF ABSTRACT	20. LIMITATION OF ABSTRACT
Unclassified	Unclassified	Unclassified	